Published in final edited form as:
J Am Chem Soc. 2010 May 5; 132(17): 6075–6080. doi:10.1021/ja909652q.

Suborganelle Sensing of Mitochondrial cAMP-Dependent Protein Kinase Activity

Richard S. Agnes[§], **Finith Jernigan**[†], **Jennifer R. Shell**[†], **Vyas Sharma**[†], and **David S. Lawrence**[†]

David S. Lawrence: lawrencd@email.unc.edu

[§]Department of Biochemistry, Albert Einstein College of Medicine, Bronx, NY 10461

[†]Department of Chemistry, Division of Medicinal Chemistry and Natural Products, Department of Pharmacology University of North Carolina, Chapel Hill, NC, 27599

Abstract

A fluorescent sensor of protein kinase activity has been developed and used to characterize the compartmentalized location of cAMP-dependent protein kinase activity in mitochondria. The sensor functions via a phosphorylation-induced release of a quencher from a peptide-based substrate, producing a 150-fold enhancement in fluorescence. The quenching phenomenon transpires via interaction of the quencher with Arg residues positioned on the peptide substrate. Although the cAMP-dependent protein kinase is known to be present in mitochondria, the relative amount of enzyme positioned in the major compartments (outer membrane, intermembrane space, and the matrix) of the organelle is unclear. The fluorescent sensor developed in this study was used to reveal the relative matrix:intermembrane space:outer membrane (85:6:9) distribution of PKA in bovine heart mitochondria.

Protein kinases are a large enzyme family that have been implicated in nearly every cell-based behavior, from ATP generation to unrestrained growth and division.1 These enzymes are linked by their ability to catalyze phosphoryl transfer from ATP to the hydroxyl moieties of serine, threonine, and/or tyrosine residues in proteins. A variety of factors limit protein kinase-catalyzed phosphorylation to intended protein targets: (a) the ability to phosphorylate serine/threonine or tyrosine, but only rarely both aliphatic and aromatic residues, (b) differential expression as a function of cell type, (c) recognition of specific amino acid sequences encompassing the hydroxyl phosphoryl acceptor moiety, and (d) localization to specific intracellular sites. The cAMP-dependent protein kinase (PKA) exhibits many of these attributes as a serine/threonine-specific protein kinase with a special preference for sequences of the general form Arg-Arg-Xaa-Ser/Thr-Xaa in protein substrates.2 In addition, PKA is anchored to a variety of intracellular sites via coordination to A-Kinase Anchoring Proteins (AKAPs), and thus the biological consequences of its action are location-dependent.3 For example, mitochondrial PKA is implicated in the regulation of apoptosis and ATP synthesis.4 However, as is true for protein kinases in general, presumed intracellular PKA activity is commonly assessed in an indirect fashion: either by the mere presence of the enzyme (immunofluorescence or western blots) or by the effect of small molecule modulators, such as inhibitors, on the phosphorylation of *presumed* PKA protein substrates. Unfortunately, these commonly employed methods don't furnish a direct measure of kinase activity.

Correspondence to: Vyas Sharma; David S. Lawrence, lawrencd@email.unc.edu.

SUPPORTING INFORMATION. This information is available free of charge via the Internet at http://pubs.acs.org/.

Fluorescent sensors have been used to directly and continuously assess kinase action.[5] However, these either display a limited dynamic range or employ fluorophores with photophysical properties (short $\lambda_{ex}/\lambda_{em}$6, small ε,7 low Φ) that are incompatible (due to interference from autofluorescence) with cells, cell lysates, or organelles. With the latter limitation in mind, we report herein the application of a quenched fluorescence strategy6 to create a kinase sensor of unprecedented dynamic range. Sensors with a large dynamic range can be used in relatively small quantities, thereby diminishing the likelihood of interference with ongoing biochemical processes (i.e. Observer Effect).8 The favorable properties associated with the sensor have allowed us to assess the relative abundance of PKA in the major mitochondrial microenvironments (outer membrane, intermembrane space, and matrix).9–13

Results and Discussion

The fluororophores described in this report are coumarin derivatives, which possess photophysical properties (Table 1) that are readily amenable to biological applications. Three coumarin-derivatized peptides (**1** – **3**; Figure 1) of the general form coumarin-Aoc-GRTGRRFSYP-amide were prepared (where Aoc = aminooctanoic acid). These positively charged peptides were exposed to forty-seven different negatively charged dyes (Supporting Information, Table S1) with the expectation that complex formation would result in the quenching of coumarin fluorescence. In addition, we anticipated that PKA-catalyzed phosphorylation of coumarin-Aoc-GRTGRRFSYP-amide would promote association of the phosphorylated peptide with the 14-3-3 domain[14], thereby releasing the quenching dye and restoring fluorescence (Scheme 1). The lead quencher dye for all three peptides proved to be Acid Green 27 (**4**) and the observed PKA-catalyzed changes in fluorescence in the presence of **4** are: peptide **1** (152-fold), peptide **2** (150-fold), and peptide **3** (28-fold) (Table 1 and Figure 2). Given its large dynamic range and relatively high V_{max} (Table 1), we decided to employ peptide **1** in all subsequent studies.

We confirmed that phosphoryl transfer from ATP to the serine hydroxyl moiety of the peptide sensor is required for the observed fluorescent enhancement by examining analogs of the peptide substrate **1** and ATP. First, substitution of peptide **1** with by its non-phosphorylatable Ala-for-Ser counterpart **5** fails to elicit a change in fluorescence (Figure 2D). Second, substitution of ATP with the corresponding thio-derivative, ATP(γ)S, dramatically reduces the rate of fluorescence change (Supporting Information, Figure S1). ATP(γ)S is known to serve as a weak thiophosphoryl donor in protein kinase-catalyzed reactions.[15,16]

Both 14-3-3 and the fluorescent quencher, Acid Green 27 (**4**), are required for the large phosphorylation-induced fluorescence yield. In the absence of 14-3-3 (but with quencher **4** present), no change in fluorescence is observed (Supporting Information, Figure S2). Furthermore, there exists a direct correlation between the relative amount of 14-3-3 present and the observed phosphorylation-dependent fluorescent enhancement (Supporting Information, Figure S2). Surprisingly, in the absence of quencher **4** (but with 14-3-3 present), there is a 50% *decrease* in observed fluorescence (Supporting Information, Figure S3). One possible explanation for the unexpected fluorescent decrease is the likely orientation of the 14-3-3-bound phospho-peptide **1** based on a previously described crystal structure.[17] The N-terminus of the peptide, when complexed with the 14-3-3 domain, is positioned adjacent to two tryptophan residues (Supporting Information, Figure S4). We,[18] as well have others,[19] have shown that tryptophan can serve as a fluorescent quencher. 14-3-3 domain-mediated quenching of phosphocoumarin-peptide fluorescence is intriguing since it suggests that removal of the tryptophan residues in the 14-3-3 domain could furnish fluorescence fold changes even larger than those observed in this study.

We examined the underlying assumption that the negatively charged quencher **4** engages the positively charged peptide substrate via electrostatic interactions. A small library of Arg-to-Ala substituted peptide analogs were prepared and K_D values were acquired for each of these with Acid Green 27, using fluorescence quenching as an indicator of complex formation. As is clear from Table 2, the quenching phenomenon is Arg residue-dependent, with the apparent K_D displaying an approximate two orders of magnitude loss for every Arg replaced by an Ala. The effect is independent of the site of the Ala-for-Arg substitution (cf. **6** vs. **7** vs. **8**), implying a diffuse electrostatic interaction between the negatively charged dye and the peptide substrate. Job plot analysis revealed the formation of a 1:1 complex between **1** and **4** (Figure 3).

The large fluorescent dynamic range of the PKA-catalyzed phosphorylation of peptide **1** furnishes a sensitive measure of kinase activity. The catalytic activity of PKA at a concentration as low as 160 pM can be detected as demonstrated by the plot of initial rate versus PKA concentration (Figure 4). Figure 4 provides a standard curve for assessing “PKA activity equivalents” in biological systems.

Although the indispensable nature of the PKA signaling pathway in mitochondrial physiology is beyond dispute,[4] its suborganelle location within the mitochondria (i.e. matrix, intermembrane space, and/or on the outer membrane oriented toward the cytoplasm; Figure 5) is enigmatic. Orr and colleagues demonstrated (via electron microscopy) that type II PKA is primarily associated with the outer membrane of mitochondria in male germ cells.[20] Indeed, a major mitochondrial A-Kinase Anchoring Protein (AKAP121 in mice and AKAP149 in humans), and its splice variants, position PKA on the cytoplasmic face of the outer membrane. 11 Proteolysis of this AKAP21,22 appears to promote apoptosis by releasing PKA from the outer membrane, which is known to promote anti-apoptotic behavior23,[24]. By contrast, Schwoch et al showed (via electron microscopy) that both types I and II PKA are primarily associated with the mitochondrial matrix/inner membrane in mitochondria isolated from a wide variety of organs.12 Matrix localization of PKA has also been observed in neuronal mitochondria.13 Papa and his colleagues found that PKA is associated with the inner membrane of bovine heart mitochondria.25 Furthermore, these investigators reported a detailed electron microscopic analysis of rat heart mitochondria and concluded that more than 90% of all mitochondrial-bound PKA is present in the inner mitochondrial compartment.10 However, an additional complication, not described by these studies, is the enzymatic reach of PKA. In particular, the majority of mitochondrial proteins are nuclear encoded and thus must be imported from the cytoplasm. Consequently, although a variety of mitochondrial proteins are phosphorylated in a cAMP-dependent fashion, they may suffer PKA-catalyzed phosphorylation during import (e.g. at the outer membrane), and thus prior to being embedded within their final destination (e.g. in the matrix).[25] In short, the mitochondrial location of known PKA substrates is not necessarily a valid indicator of microenvironmental PKA activity. Finally, the active form of PKA (C subunit), which is released from the inactive holoenzyme (R_2C_2) upon exposure to cAMP, can diffuse through membranes.[26] Therefore, the suborganelle location of the holoenzyme (as determined by electron microscopy) does not necessarily recapitulate the location of the active form of the enzyme. With these factors in mind, we turned our attention to the suborganelle analysis of cAMP-activated PKA in isolated bovine heart mitochondria.

Perhaps the most obvious approach for assessing PKA activity as a function of mitochondrial microenvironment is purification of the enzyme from the outer membrane, the intermembrane space, and the matrix. However, such a strategy is not practical for both structural and technological reasons. The holoenzyme resides as an AKAP-bound membrane-associated species on the outer membrane and likely, in an analogous AKAP-dependent fashion, at the inner membrane. Unfortunately, even if it were feasible to isolate and purify the outer and inner membrane components, it would not be clear which direction the enzyme is facing in the intact

mitochondrion (i.e. an outer membrane-bound species could be oriented outward toward the cytoplasm or inward toward the intermembrane space). An alternative approach might involve the cAMP-induced release of the C subunit and its subsequent isolation from the extramitochondrial, intermembrane space, and matrix regions. However, as demonstrated with bovine heart mitochondria, the standard technique used to expose the contents of the intermembrane space (digitonin treatment) results in some disruption of the matrix as well, leading to contamination of the intermembrane space contents with components from the matrix.[27] Therefore, we resorted to the strategy depicted in Figure 5.

We reasoned that exposure of intact mitochondria to cAMP should activate PKA located on the outer membrane as well as any PKA present in the intermembrane space (i.e. inner leaflet of the outer membrane and/or outer leaflet of the inner membrane). The mitochondrial outer membrane contains a channel forming protein-based complex (porin; also known as the voltage dependent anion channel) that allows small molecules (<5000 molecular weight) to passively diffuse between the extramitochondrial environment and the intermembrane space.[28] We expected that, in addition to cAMP, our PKA sensor **1** and quencher **4** should be able to freely migrate into and out of the intermembrane space and thus report any PKA activity (by contrast, the inner membrane blocks access to the matrix of externally added cAMP29). This approach avoids the use of digitonin, and thus should prevent contamination by the unintended release of matrix contents. In short, cAMP-treated mitochondria should furnish outer membrane *and* intermembrane space PKA activity. Furthermore, since trypsin digests only outward-facing outer membrane mitochondrial proteins,[9] we expected that cAMP-exposed *trypsin*-treated mitochondria should provide only intermembrane space PKA activity (Figure 5). Finally, mitochondrial structural integrity is completely disrupted by sonication and thus mitochondria treated in this fashion should yield, upon cAMP exposure, total mitochondrial PKA activity. These three activities can then be used to assign relative PKA activity to the three separate mitochondrial microenvironments.

The purity of mitochondria isolated from bovine heart was assessed via Western blot analysis using antibodies against proteins that are localized to mitochondrial (cytochrome C) and non-mitochondrial sites, including the endoplasmic reticulum (calnexin), the plasma membrane (Na^+/K^+ ATPase), and the cytosol (GAPDH) (Figure 6A). The results demonstrate that the mitochondrial preparation is not contaminated with proteins from other membranes or the ER, and displays only minimal contamination from the cytoplasm. Mitochondrial structural integrity (intactness) was assessed as previously described30,31 and found to be greater than 90% (data not shown).

Intact mitochondria, upon exposure to cAMP, exhibit an initial rate of PKA activity equivalent to 29 ± 4 pg PKA/μg mitochondria. By contrast, in the absence of cAMP, phosphorylation activity is minimal (Supporting Information, Figure S5); demonstrating that sensor **1** is phosphorylated in a cAMP-dependent fashion. Indeed, previous studies have shown that active site directed sequences, similar to the sequence employed in sensor **1**, are highly selective for PKA.[32–34] Finally, we have found that H-89, a PKA inhibitor, blocks the phosphorylation of sensor **1** by mitochondrial preparations (Supporting Information, Figure S6). These results are consistent with the notion that peptide **1** serves as a selective PKA sensor.

As noted above (Figure 5), we expected that the PKA activity associated with intact mitochondria would be a combination of enzyme present on the outer membrane and enzyme oriented into the intermembrane space. We addressed this possibility by treating mitochondria with trypsin, which should selectively hydrolyze the outer membrane proteins exposed to the external milieu (Figure 6B), but not hydrolyze matrix- or intermembrane space-embedded proteins. Indeed, an outer membrane marker (TOM 20) is completely digested in trypsin-treated mitochondria, whereas a matrix marker (Hsp 60) is unperturbed. Previous studies with

trypsin-exposed mitochondria demonstrated that an intermembrane space marker is protected against proteolysis as well.[9] Subsequent analysis of PKA activity (cAMP exposure) in trypsin-treated mitochondria revealed a drop in PKA activity from 24 ± 4 pg PKA/μg mitochondria to 10 ± 1 pg PKA/μg mitochondria, implying a 1:1.4 ratio of intermembrane space:outer membrane (external) PKA. Finally, mitochondria were sonicated to completely disrupt their structural integrity, thereby exposing all mitochondria-associated PKA, including any matrix-embedded enzyme. Total mitochondrial PKA activity (cAMP treatment) is equivalent to 165 ± 24 pg PKA/μg mitochondria, approximately 5.7 times greater than that observed with intact mitochondria. These values suggest that the relative distribution of PKA activity in the matrix (165 ± 24 pg PKA/μg mitochondria − 24 ± 4 pg PKA/μg mitochondria = *141 pg PKA/μg mitochondria*), the intermembrane space (*10 ± 1 pg PKA/μg mitochondria*), and the outer membrane (24 ± 4 pg PKA/μg mitochondria − 10 ± 1 pg PKA/μg mitochondria = *14 pg PKA/μg mitochondria*) in bovine heart mitochondria is 85:6:9, respectively. The latter compares favorably with the electron microscopy work of Papa and colleagues,[10] who reported that 90% of the PKA present in mitochondria is found the matrix and the intermembrane space. However, our analysis could be complicated by endogenous protein phosphatases if they are present in different amounts in the three distinct mitochondrial compartments. Consequently, an analogous series of experiments were conducted in the presence of a phosphatase inhibitor cocktail. The experimentally determined ratio (79:8:13) of matrix:intermembrane space:outer membrane PKA activity corresponds to that acquired in the absence of phosphatase inhibitors.

In summary, we have developed a protein kinase sensing system with a robust dynamic range and used it to characterize the compartmentalized location of PKA activity in mitochondria. Given the important role of PKA in mediating the dynamics of mitochondrial biochemistry, the ability to monitor protein kinase activity should prove useful in assessing the mitochondrial response from both healthy individuals and from patients with mitochondrial-based disorders.[35]

Materials and Methods

Materials

General reagents and solvents were purchased from Fisher or Sigma-Aldrich. Novasyn TGR Resin, all natural Fmoc-protected amino acids were purchased from EMD Biosciences Inc. HCTU [1H-benzotriazolium 1-[bis(dimethylamino)methylene]-5-chloro-hexafluorophosphate (1-),3-oxide] was purchased from Peptides International (Louisville, KY). Fluorescent dyes (7-(diethylamino)coumarin-3-carboxylic acid, Coumarin 343 [11-oxo-2,3,6,7-tetrahydro-1H,5H,11H-pyrano[2,3-f]pyrido[3,2,1-ij]quinoline-10-carboxylic acid], and Atto 425-NHS ester were purchased from Sigma-Aldrich. Fmoc-aminooctanoic acid (Fmoc-Aoc-OH) was purchased from Advanced ChemTech (Louisville, KY). Bovine heart mitochondria was purchased from MitoSciences and trypsin (sequencing grade) and PKA were purchased from Promega. The antibodies against the PKA catalytic subunit, Tom 20, and Hsp60 were purchased from BD Biosciences and the goat anti-mouse secondary antibody was purchased from Santa Cruz Biotechnology. Total mitochondrial protein was quantified using the BCA protein assay (Pierce). Immunoblots were performed using Snap i.d. (Millipore), and visualized using an AlphaInnotech FluorChem FC2 imager. The intactness of the isolated mitochondria was assessed via a previously described protocol.[30,31] PKA murine catalytic subunit (cat) plasmid and the GST-14-3-3τ plasmid were generous gifts from Dr. Susan Taylor and Dr. Alistair Aitken, respectively.

Synthesis of fluorophore-labeled PKA substrates

Peptides were synthesized using standard Fmoc solid phase synthesis on a Prelude peptide synthesizer (Protein Technologies Inc, Tucson, Az). Novasyn TGR resin was swelled for 30

min in dichloromethane (DCM) before synthesis. Amino acids were then sequentially coupled using 5.0 equiv. amino acid, 4.9 equiv. HCTU, 20 equiv. diisopropylethylamine (DIPEA) in N,N-dimethylformamide (DMF) (2 × 5 min) followed by DMF wash (6 × 30 s). The Fmoc-protecting group was removed using 20% piperidine in DMF (2 × 2.5 min) followed by a DMF wash (6 × 30 s). The free N-terminal amine was used for subsequent on-resin fluorophore labeling. Fluorescent dyes diethylcoumarin and Coumarin 343 were coupled to the N-terminal amine using 5.0 equiv. fluorophore, 4.9 equiv. HCTU, 20 equiv. DIPEA in DMF (1× 60 min). Atto425-NHS ester was coupled using 1.0 equiv. dye and 20 equiv. DIPEA in DMF (1 × 60 min). The resin was washed (3× DMF, IPA, DCM) and then cleaved and deprotected using a 95:2.5:2.5 mixture of trifluoroacetic acid (TFA), H_2O, and triisopropylsilane (TIPS). The peptides were isolated via filtration, precipitated with ice-cold ether, and centrifuged to isolate the precipitate. The precipitates were air-dried, dissolved in DMSO, and purified using HPLC (3% – 40% acetonitrile gradient against water with 0.1% TFA over 40 min). The peak corresponding to the peptide was collected, freeze dried, and characterized by electrospray ionization mass spectrometry: **1** Cou-Aoc-GRTGRRFSYP-amide [Exact Mass calculated: 1579.84, found: 1580.84 $(M + H)^+$], **2** Atto425-Aoc-GRTGRRFSYP-amide [Exact Mass calculated: 1719.98, found: 1720.97 $(M+H)^+$], **3** Cou343-Aoc-GRTGRRFSYP-amide [Exact Mass calculated: 1603.82, found: 1604.85 $(M+H)^+$], **5** Cou-Aoc-GRTGRRFAYP-amide [Exact Mass calculated: 1562.8, found: 782.6 $(M+2H)^{2+}$, 522.2 $(M+3H)^{3+}$], **6** Cou-Aoc-GATGRRFSYP-amide [Exact Mass calculated: 1494.69, found: 1495.80 $(M+H)^+$], **7** Cou-Aoc-GRTGARFSYP-amide [Exact Mass calculated: 1494.69, found: 1495.77 $(M+H)^+$], **8** Cou-Aoc-GRTGRAFSYP-amide [Exact Mass calculated: 1495.69, found: 1495.78 $(M+H)^+$], **9** Cou-Aoc-GATGRAFSYP-amide [Exact Mass calculated: 1409.58, found: 1409.72 $(M+H)^+$], **10** Cou-Aoc-GATGARFSYP-amide [Exact Mass calculated: 1409.58, found: 1409.73 $(M+H)^+$], **11** Cou-Aoc-GRTGAAFSYP-amide [Exact Mass calculated: 1409.58, found: 1409.72 $(M+H)^+$], and **12** Cou-Aoc-GATGAAFSYP-amide [Exact Mass calculated: 1323.6, found: 1324.5 $(M+H)^+$].

Identification of lead quencher dye 4

The concentration of peptide **1** was adjusted using a molar excitation coefficient of 60,000 M^{-1} cm^{-1} at 430 nm. GST-tagged 14-3-3 (purified to a single band at 56 KDa on 12.5% SDS PAGE) was dialyzed four times in 50 mM Tris pH 7.5, prior to use, and its concentration was determined using the Bradford assay. Concentrations of each of the forty-seven assembled dyes (See Table S1) were adjusted based on weight. PKA enzyme (2.08 mg/mL) was purchased from Promega. 1 μM peptide **1** was incubated with 10 μM GST-tagged 14-3-3, 1 mM ATP, 2 mM DTT, 5 mM $MgCl_2$ and 50 mM Tris-HCl at pH 7.5, in a quartz 96 well plate (Hellma). Each dye was added to a separate well at 5 μM. 10 nM PKA was added per well and enzyme-dependent increase in fluorescence (λ_{ex} 420 nm, λ_{em} 475 nm) was determined with a plate reader (Molecular Devices Spectra Max Gemini EM). Dyes D1, D6, D18, D33 and D39 showed >2 fold enhancements in fluorescence.

Phosphorylation of Sensor 1 and dephosphorylation of phospho-sensor peptide

PKA-catalyzed phosphorylation of sensor **1** was performed using the conditions in "Optimization of enzyme-dependent fold-change" described below. The mass of the resulting phosphorylated peptide was found to be 830.6 $(M + 2H)^{2+}$, 554.1 $(M + 3H)^{3+}$ (Exact Mass calculated 1658.8). The phosphorylated lead peptide was dephosphorylated using Protein Phosphatase 1 (NEB) in the presence of 50 mM HEPES pH 7.5, 100 mM NaCl, 2 mM DTT, 0.01 % Brij 35, and 1 mM $MnCl_2$. The mass of the resulting dephosphorylated peptide was found to be 789.5 $(M + 2H)^{2+}$ (Exact Mass calculated 1577.8).

Acquisition of apparent K_m and V_{max} values

Phosphorylation-dependent increase in coumarin fluorescence intensity of peptides **1** – **3** was monitored on a Photon Technology QM-1 spectrofluorimeter at 30 °C. Standard curves were used to correlate fluorescence intensity with concentration of product formed. For generating the standard curve, various substrate concentrations were incubated, in duplicate, with 5 nM PKA at 25 °C over 30 h (in the presence of 320 μM dye, 20 μM 14-3-3τ, 1 mM ATP, 5 mM $MgCl_2$, 2 mM DTT and 50 mM Tris HCl pH 7.5). The fluorescence intensity after complete phosphorylation was plotted against concentration, and parameters obtained from a linear regression of the data were used to convert the fluorescence intensity to product concentration. For determining the initial velocities, different concentrations of the peptide substrate was equilibrated with 20 μM 14-3-3τ, 1 mM ATP, 5 mM $MgCl_2$, 2 mM DTT, in 50 mM Tris buffer pH 7.5, for 10 min. PKA (5 nM) was added and the reaction progress curves obtained. Reaction rates were determined from the slope under conditions where 5 – 8% substrate had been converted to product in duplicate (typically from 200 – 300 s). The resulting slopes (initial velocity, v_o) for each of the progress curves were plotted versus the concentration of substrate. A nonlinear regression analysis (SigmaPlot version 8.02 software) was used to fit the data to the rectangular hyperbola model.

Optimization of enzyme-dependent fold-change

1 μM peptide **1** was incubated with 1 mM ATP, 2 mM DTT, 5 mM $MgCl_2$, 50 mM Tris-HCl at pH 7.5, in different wells of a quartz 96-well plate. To each well, systematically varied concentrations of dye **4** (0 – 600 μM) and GST-tagged 14-3-3 (0 – 40 μM) were added followed by 10 nM PKA. Enzyme dependent enhancement in fluorescence (λ_{ex} 420 nm, λ_{em} 475 nm) was determined with a plate reader (Molecular Devices Spectra Max Gemini EM). The maximum fluorescence increase was observed with 320 μM dye **4** and 20 μM GST-tagged 14-3-3τ. These optimized conditions were used to assay peptides **1** – **3** using a Photon Technology QM-4 spectrofluorimeter. The enzyme dependent fold changes obtained under these conditions are reported in Table 1 and are shown in Figure 2.

Acquisition of apparent K_d values for 4 with peptides 1 and 6 – 12

Varying concentrations of **4** ranging from 0.02 – 200 μM, were added to 1 μM of the coumarin-labeled peptides in 100 mM Tris HCl pH 7.5 buffer. Fluorescence data (λ_{ex} 420 nm, λ_{em} 475 nm) was acquired using a Photon Technology QM-4 spectrofluorimeter at 30 °C. Correction for the inner filter effect was made as previously reported.[36] Molar absorbtivities (λ_{ex} 420 nm, λ_{em} 475 nm) were calculated from single absorbance spectra at a [**4**] = 16 μM. After correcting for the inner filter effect, the percentage of quench was plotted against the concentration of the dye. Concentration of the dye-peptide complex was determined based on the change in fluorescence emission intensity. The data was fit using the non-linear regression mode of SigmaPlot ver.8.02. The calculated K_d values are reported in Table 2.

Job plot for determination of stoichiometry

Fluorescence emission (λ_{ex} 420 nm, λ_{em} 475 nm) of varying concentrations of peptide **1** (0.2 μM, 0.6 μM, 1.0 μM, 1.4 μM, 1.8 μM) and dye **4** (65% purity) (1.8 μM, 1.4 μM, 1 μM, 0.6 μM, 0.2 μM) at a fixed total concentration of 2 μM was acquired in duplicate, on a Photon Technology QM-4 spectrofluorimeter at 30 °C (Figure 3).

Mitochondria-based experiments

A standard curve for PKA concentration versus activity was generated using 1 μM peptide **1**, 32 μM dye **4**, 10 μM 14-3-3τ, 1 mM ATP, 5 mM $MgCl_2$, 2 mM DTT, 1 mM cAMP, in 50 mM Tris HCl at pH 7.5. Assays were conducted in duplicate at two concentrations of total mitochondria protein (14 μg and 55 μg) using intact mitochondria (MitoSciences), trypsin-

treated mitochondria (mitochondria samples incubated with 1:50 trypsin:total mitochondrial protein for 1 h at 37° C, followed by treatment with 20-fold excess of soybean trypsin inhibitor) and sonicated mitochondria, [mitochondria sonicated (Ultrasonic Processor, Tekmar, Cincinnati, OH, USA) for 30 s on ice]. Initial rates were converted into pg of active PKA per μg of mitochondria using the standard curve. Rates in the presence of Ser/Thr Phosphatase inhibitor cocktail (P2850 Sigma) were acquired at the recommended 1:100 dilution.

Trypsin treatment of mitochondria

Mitochondria were incubated with trypsin (1:50 trypsin:total mitochondrial protein) for 1 h at 37° C followed by treatment with a 20-fold excess of soybean trypsin inhibitor. The outcome of the trypsin digestion was validated by Western blot using an outer membrane marker, Tom 20, and a matrix marker, Hsp60.

Western blot analyses

20 μg of total protein was loaded onto 4 – 12% bis-tris polyacrylamide gels, separated by electrophoresis, and electroblotted onto PVDF membranes. The membranes were then blocked in 0.5% nonfat dry milk followed by incubation with the appropriate primary antibody (C subunit of PKA 1:1000, Tom 20 1:1000, and Hsp60 1:5000) for 10 min. The membranes were then washed 3 times with 0.1% Tween-20 in PBS followed by incubation with a goat anti-mouse secondary antibody conjugated to horseradish peroxidase (1:2000) for 10 min. The membranes were washed with 0.1% Tween-20 in PBS (3×), PBS (3×), and 0.5% NaCl (3×) and detection of horseradish peroxidase performed using the ECL Plus reagent (GE).

Supplementary Material

Refer to Web version on PubMed Central for supplementary material.

Acknowledgments

We thank the NIH (CA79954 and NS048406) for financial support.

References

1. Manning G, Whyte DB, Martinez R, Hunter T, Sudarsanam S. Science 2002;298:1912–1934. [PubMed: 12471243]
2. Shabb JB. Chem Rev 2001;101:2381–2411. [PubMed: 11749379]
3. Smith FD, Langeberg LK, Scott JD. Trends Biochem Sci 2006;31:316–323. [PubMed: 16690317]
4. Feliciello A, Gottesman ME, Avvedimento EV. Cell Signal 2005;17:279–287. [PubMed: 15567059]
5. Lawrence DS, Wang Q. Chembiochem 2007;8:373–378. [PubMed: 17243187]
6. Sharma V, Agnes RS, Lawrence DS. J Am Chem Soc 2007;129:2742–2743. [PubMed: 17305340]
7. Shults MD, Imperiali B. J Am Chem Soc 2003;125:14248–14249. [PubMed: 14624552]
8. Sharma V, Lawrence DS. Angew Chem Int Ed Engl 2009;48:7290–7292. [PubMed: 19739174]
9. Ma Y, Taylor SS. J Biol Chem 2008;283:11743–11751. [PubMed: 18287098]
10. Sardanelli AM, Signorile A, Nuzzi R, Rasmo DD, Technikova-Dobrova Z, Drahota Z, Occhiello A, Pica A, Papa S. FEBS Lett 2006;580:5690–5696. [PubMed: 16996504]
11. Chen Q, Lin RY, Rubin CS. J Biol Chem 1997;272:15247–15257. [PubMed: 9182549]
12. Schwoch G, Trinczek B, Bode C. Biochem J 1990;270:181–188. [PubMed: 2396978]
13. Ryu H, Lee J, Impey S, Ratan RR, Ferrante RJ. Proc Natl Acad Sci U S A 2005;102:13915–13920. [PubMed: 16169904]
14. Yaffe MB, Rittinger K, Volinia S, Caron PR, Aitken A, Leffers H, Gamblin SJ, Smerdon SJ, Cantley LC. Cell 1997;91:961–971. [PubMed: 9428519]
15. Zou K, Cheley S, Givens RS, Bayley H. J Am Chem Soc 2002;124:8220–8229. [PubMed: 12105899]

16. Anderson MP, Berger HA, Rich DP, Gregory RJ, Smith AE, Welsh MJ. Cell 1991;67:775–784. [PubMed: 1718606]
17. Rittinger K, Budman J, Xu J, Volinia S, Cantley LC, Smerdon SJ, Gamblin SJ, Yaffe MB. Mol Cell 1999;4:153–166. [PubMed: 10488331]
18. Lee HM, Priestman MA, Lawrence DS. J Am Chem Soc 132:1446–1447. [PubMed: 20073458]
19. Doose S, Neuweiler H, Sauer M. Chemphyschem 2005;6:2277–2285. [PubMed: 16224752]
20. Lieberman SJ, Wasco W, MacLeod J, Satir P, Orr GA. J Cell Biol 1988;107:1809–1816. [PubMed: 2972731]
21. Yoo H, Cha HJ, Lee J, Yu EO, Bae S, Jung JH, Sohn I, Lee SJ, Yang KH, Woo SH, Seo SK, Park IC, Kim CS, Jin YW, Ahn SK. Oncol Rep 2008;19:1577–1582. [PubMed: 18497968]
22. Carlucci A, Adornetto A, Scorziello A, Viggiano D, Foca M, Cuomo O, Annunziato L, Gottesman M, Feliciello A. EMBO J 2008;27:1073–1084. [PubMed: 18323779]
23. Affaitati A, Cardone L, de Cristofaro T, Carlucci A, Ginsberg MD, Varrone S, Gottesman ME, Avvedimento EV, Feliciello A. J Biol Chem 2003;278:4286–4294. [PubMed: 12427737]
24. Harada H, Becknell B, Wilm M, Mann M, Huang LJ, Taylor SS, Scott JD, Korsmeyer SJ. Mol Cell 1999;3:413–422. [PubMed: 10230394]
25. Papa S, Sardanelli AM, Scacco S, Technikova-Dobrova Z. FEBS Lett 1999;444:245–249. [PubMed: 10050768]
26. Harootunian AT, Adams SR, Wen W, Meinkoth JL, Taylor SS, Tsien RY. Mol Biol Cell 1993;4:993–1002. [PubMed: 8298196]
27. Burnette B, Batra PP. Anal Biochem 1985;145:80–86. [PubMed: 2988371]
28. Alberts, B.; Johnson, A.; Lewis, J.; Raff, M.; Roberts, K.; Walter, P. Molecular Biology of the Cell: Reference Edition. New York: Garland Science; 2007. p. 818
29. Acin-Perez R, Salazar E, Kamenetsky M, Buck J, Levin LR, Manfredi G. Cell Metab 2009;9:265–276. [PubMed: 19254571]
30. Wharton DC, Tzagoloff A. Methods Enzymol 1967;10:245–250.
31. Rice, JE.; Lindsay, JG. Subcellular Fractionation. Graham, JM.; Rickwood, D., editors. Oxford, England: IRL Press; 1997. p. 107-142.
32. Su J, Bringer MR, Ismagilov RF, Mrksich M. J Am Chem Soc 2005;127:7280–7281. [PubMed: 15898754]
33. Min DH, Su J, Mrksich M. Angew Chem Int Ed Engl 2004;43:5973–5977. [PubMed: 15547909]
34. He Y, Yeung ES. Electrophoresis 2003;24:101–108. [PubMed: 12652579]
35. Carlucci A, Lignitto L, Feliciello A. Trends Cell Biol 2008;18:604–613. [PubMed: 18951795]
36. Levine RL. Clin Chem 1977;23:2292–2301. [PubMed: 923078]

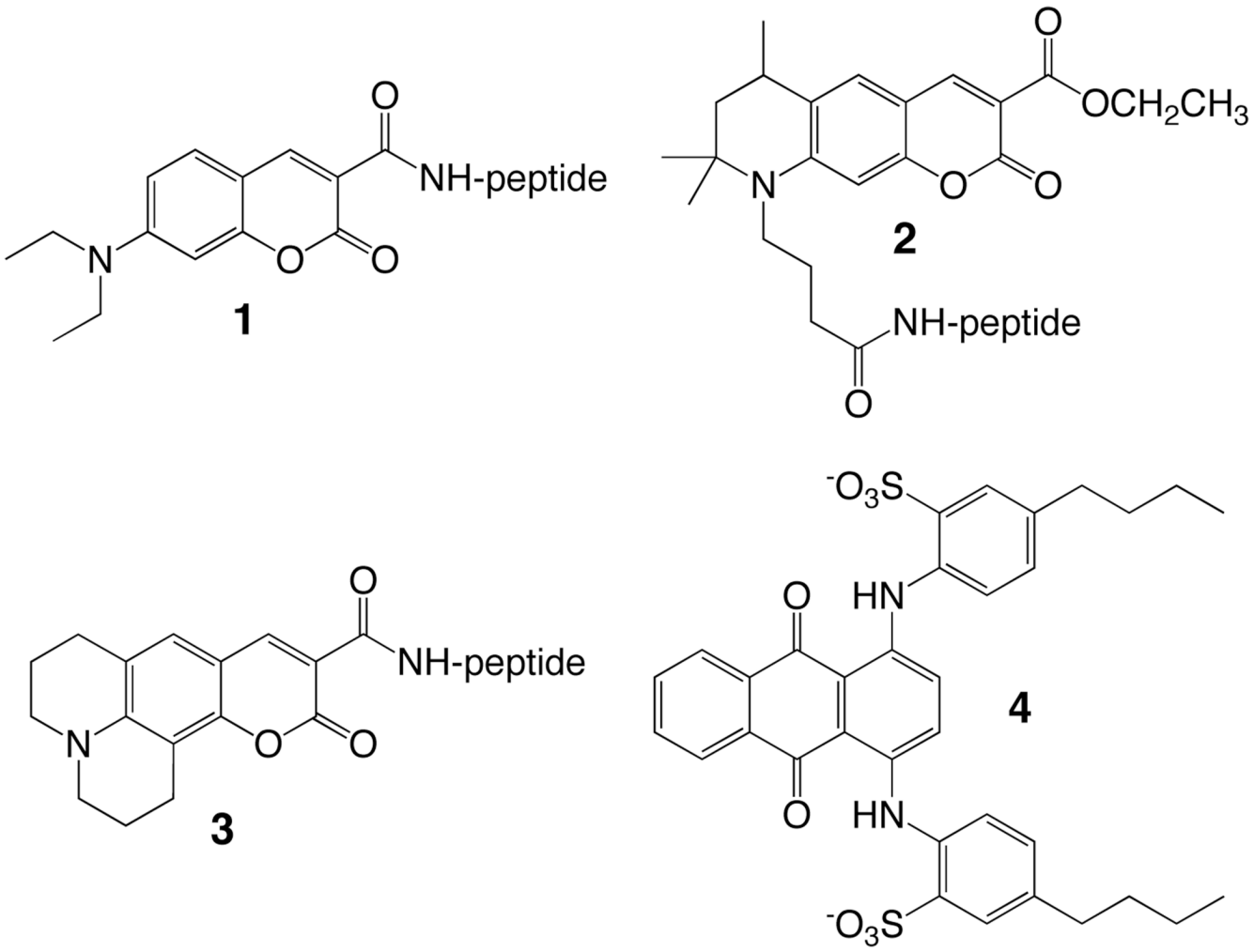

Figure 1.

Structures of the coumarin derivatives **1** – **3** of the general form fluorophore-Aoc-GRTGRRFSYP-amide. The fluorescent quencher Acid Green 27 (**4**) was identified from a library of forty-seven dyes (Table S1).

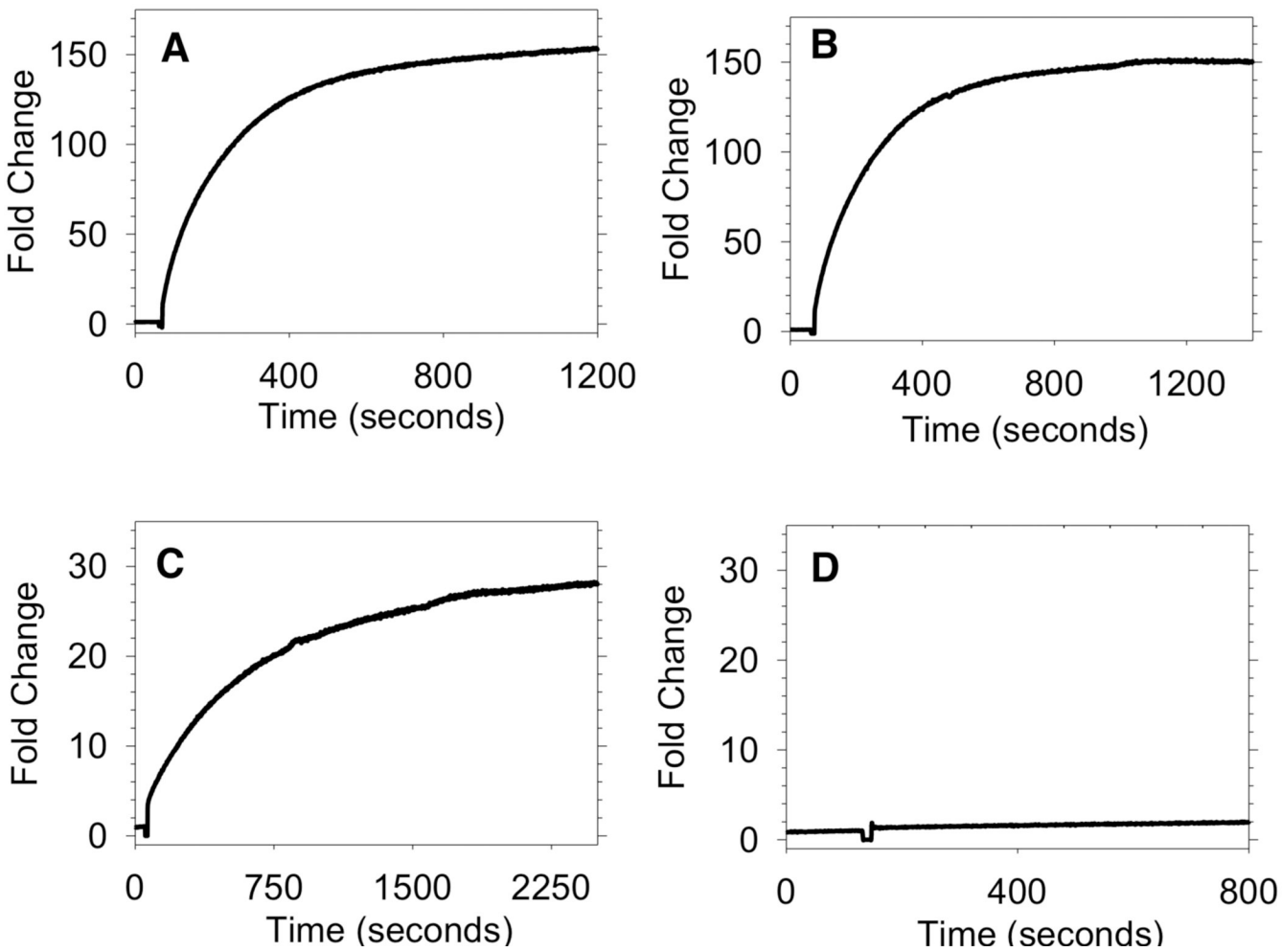

Figure 2.

Fluorescence change as a function of incubation time of the PKA-catalyzed phosphorylation of sensors (A) **1**, (B) **2**, (C) **3**, and (D) a nonphosphorylatable Ala-for-Ser control peptide **5** (coumarin-Aoc-GRTGRRFAYP-amide). Experiments were conducted in the presence of fluorescent quencher (**4**) and 14-3-3 domain. See "Optimization of enzyme-dependent fold-change" in the **Material and Methods** section for experimental details.

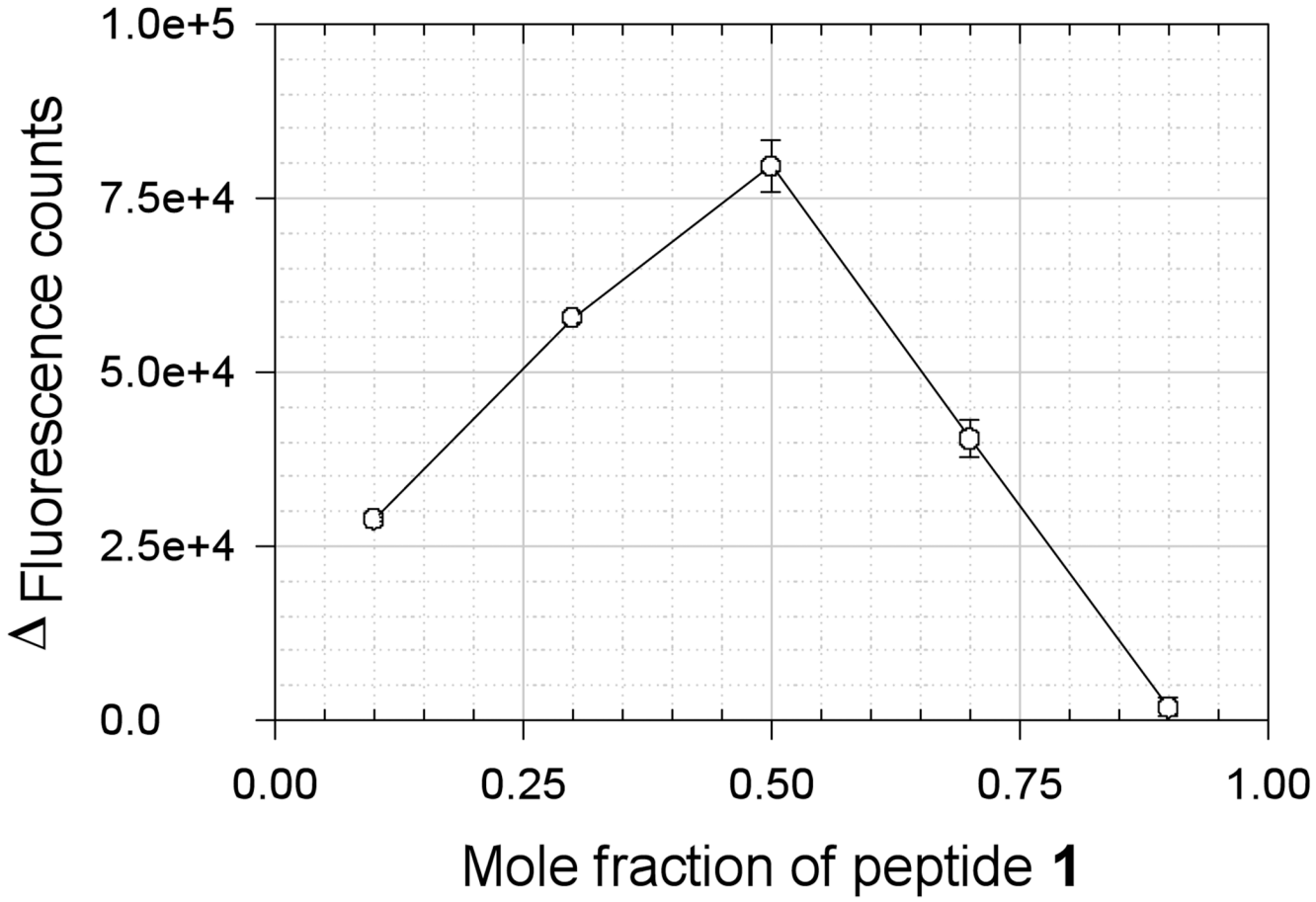

Figure 3.
Fluorescence change as a function of mole fraction of sensor **1**. See "Job plot for determination of stoichiometry" in the **Material and Methods** section for experimental details.

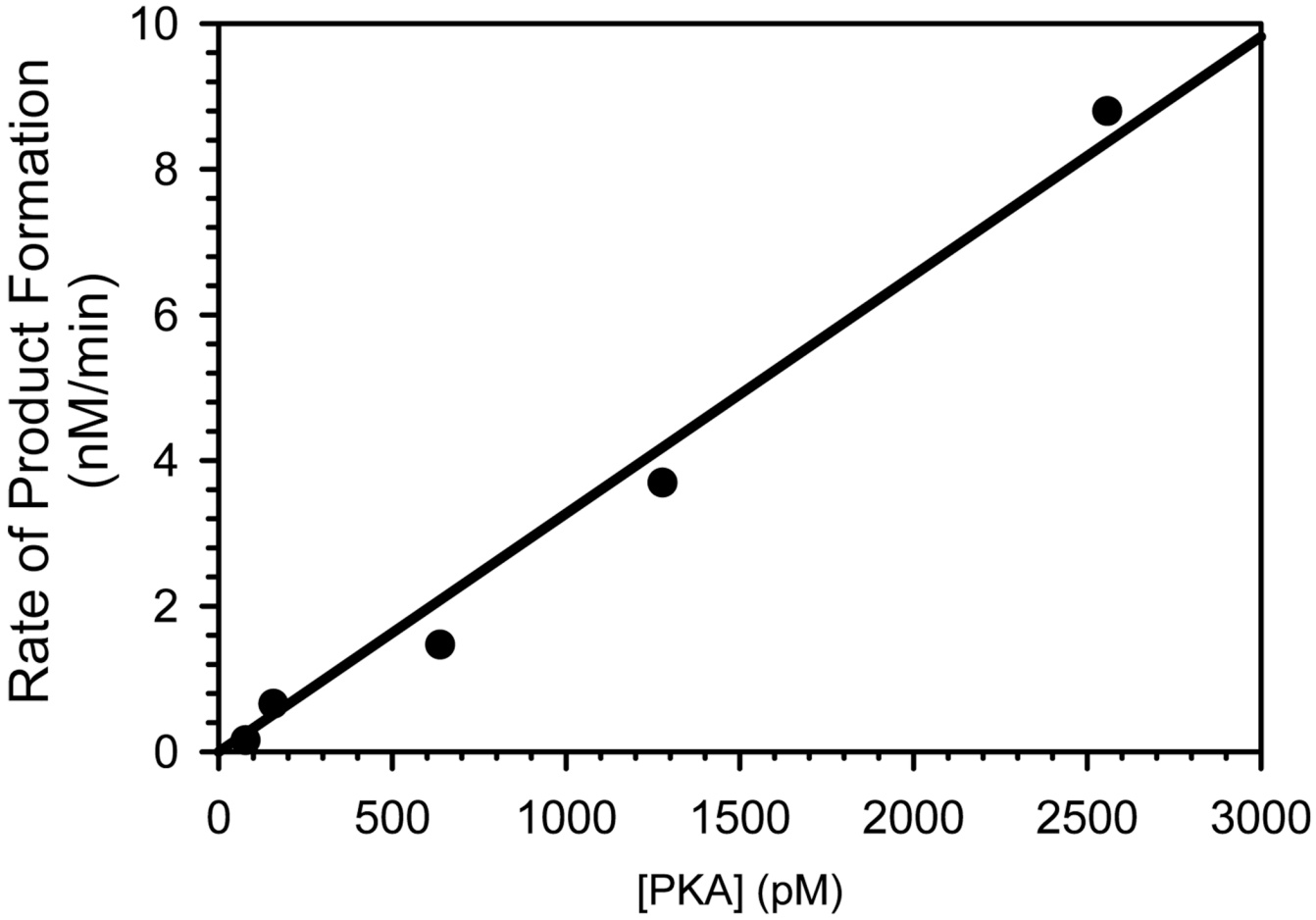

Figure 4.
Reaction rate (nM of phosphopeptide formation/min) as a function of PKA concentration (pM).

Figure 5.
Strategy for assessing PKA activity on the outer membrane (blue), in the intermembrane space (red) and in the matrix (yellow). PKA activity of intact mitochondria (**A**) is due to enzyme present on the outer membrane and in the intermembrane space. Trypsinized (i) mitochondria (**B**) lack outer membrane proteins and thus only intermembrane space PKA is present. Sonicated (ii) mitochondria (**C**) furnishes enzyme from all three compartments and thus represents total mitochondrial PKA.

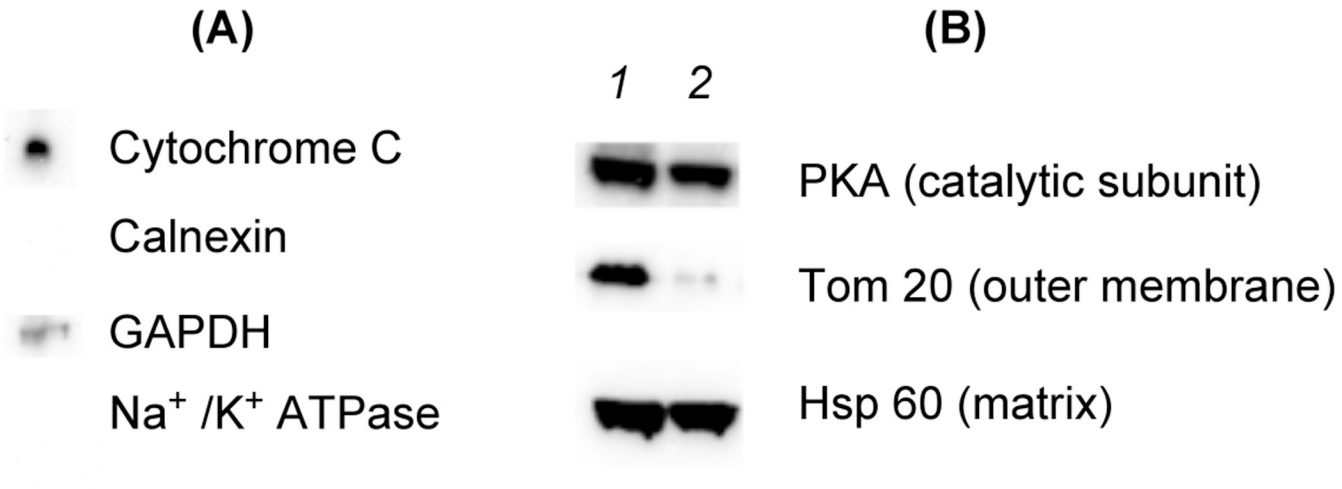

Figure 6.

Assessment of mitochondrial purity and extent of trypsinolysis by Western blot analysis. (A) The mitochondrial preparation was examined for the presence of ER (calnexin), plasma membrane (Na+/K+-ATPase), and cytoplasmic (glyceraldehyde phosphate dehydrogenase) proteins. A minimal amount of cytoplasmic contamination is observed. (B) Trypsin digestion of intact mitochondria. Untreated mitochondria (lane 1) and mitochondria treated with trypsin for 1 h at 37 °C (lane 2) were analyzed by Western blot for Hsp 60 and Tom 20, matrix and outer membrane markers, respectively, and the PKA catalytic subunit. Complete loss of Tom 20 upon trypsin exposure implies extensive trypsinolysis of the outer membrane surface. Complete retention of Hsp 60 implies that the mitochondrial matrix is preserved upon exposure to trypsin.

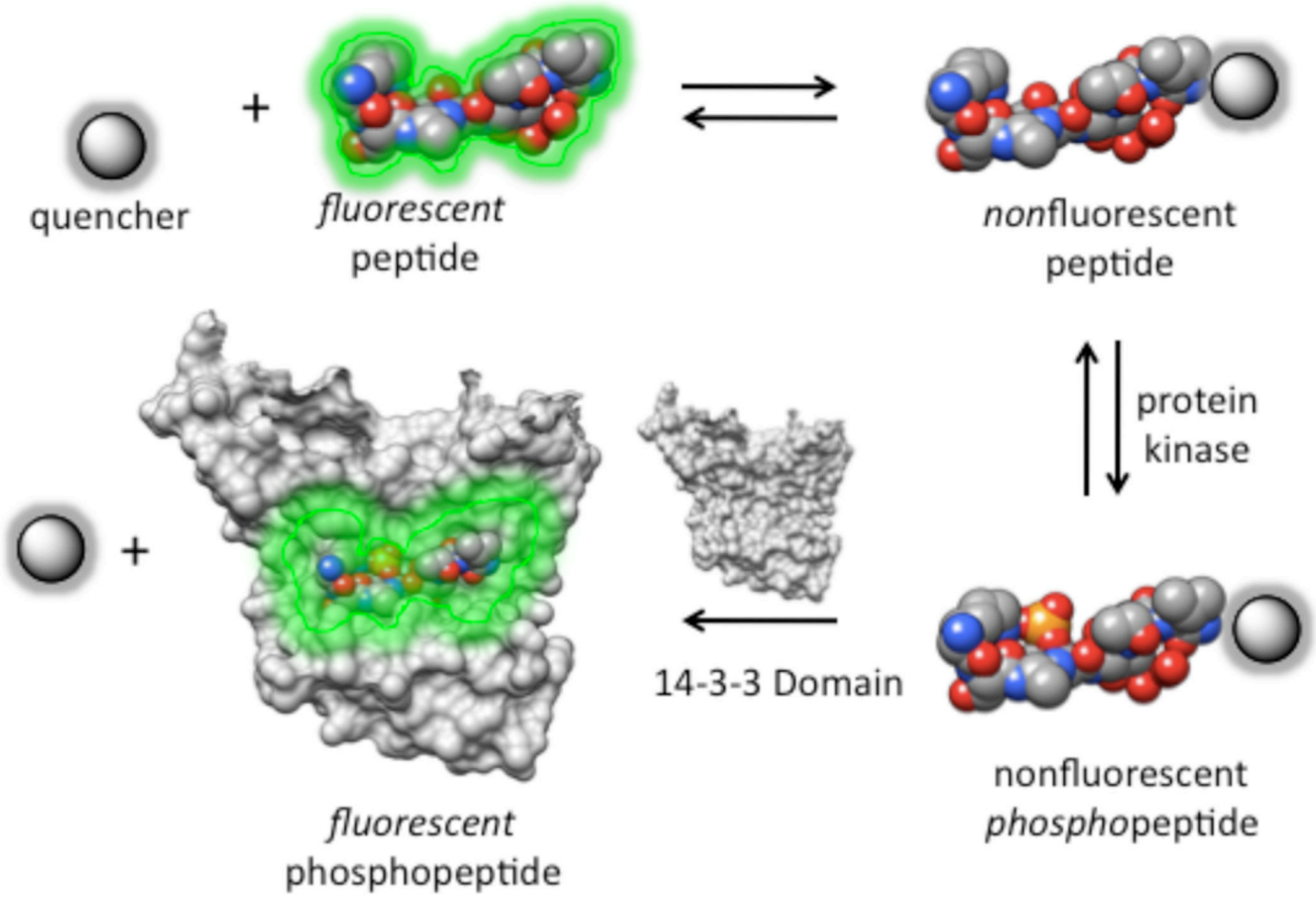

Scheme 1.
Protein kinase-catalyzed phosphorylation of a fluorescently quenched peptide generates a fluorescent response in the presence of the phosphoSer-binding 14-3-3 domain.

Table 1

Photophysical properties, fluorescent fold increase, K_m, and V_{max} for the PKA-catalyzed phosphorylation of sensors **1** – **3** (where sensor = Fluorophore-Aoc-GRTGRRFSYP-amide). Kinetic properties were acquired in the presence of quencher **4** and the 14-3-3 domain. See "Acquisition of apparent K_m and V_{max} values" in the **Material and Methods** section for experimental details.

Sensor ($\lambda_{ex}/\lambda_{em}$)	Fluorescent Fold-Increase	K_m (μM)	V_{max} (μmol/min·mg)
1 (420/475 nm)	152	2.2 ± 0.1	0.53 ± 0.03
2 (437/477 nm)	150	1.9 ± 0.1	0.34 ± 0.04
3 (450/490 nm)	28	6.2 ± 0.1	0.20 ± 0.09

Table 2

K_D values of sensor **1**, and various Ala-for-Arg analogs (**6** – **12**) of sensor **1**, with the fluorescent quencher **4**. See "Acquisition of apparent K_d values for **4** with peptides **1** and **6** – **12**" in the **Material and Methods** section for experimental details.

Peptide	Peptide Sequence	K_D (μM)
1	Cou-Aoc-GRTGRRFSYP-amide	0.04 ± 0.07
6	Cou-Aoc-G**A**TGRRFSYP-amide	1.6 ± 0.3
7	Cou-Aoc-GRTG**A**RFSYP-amide	2.7 ± 0.6
8	Cou-Aoc-GRTGR**A**FSYP-amide	1.8 ± 0.2
9	Cou-Aoc-G**A**TGR**A**FSYP-amide	130 ± 80
10	Cou-Aoc-G**A**TG**A**RFSYP-amide	130 ± 65
11	Cou-Aoc-GRTG**AA**FSYP-amide	130 ± 70
12	Cou-Aoc-G**A**TG**AA**FSYP-amide	> 200